Caving 2026 – A van As, D Cumming-Potvin & J Wesseloo (eds)

doi:10.36487/ACG_repo/2645_05

Lessons from the geotechnical reconciliation of the B3 cave

Komal Mann [a], **Yoko Yanagimura** [b], **John Hadjigeorgiou** [a,*]

[a] *University of Toronto, Canada*

[b] *Coeur Mining, Inc, Canada*

Abstract

The geotechnical design of a cave is a complex process that must anticipate considerable changes in stress demand over the life of the cave. This includes the challenges of selecting and applying appropriate design tools, as well as collecting high-quality input data to provide confidence in the analysis results. Continuous improvement of the geotechnical design approach requires reconciling predicted behaviour with observed performance. Systematic, quantitative comparison of predictions and actual responses provides insight into the performance of each design tool and highlights opportunities to refine both the tools and the overall design methodology over time.

This paper presents a case study from the B3 extraction level at the New Afton Mine that links geotechnical predictions with observed performance over the life of the cave. It outlines the numerical models, empirical methods, and accumulated site experience used to define the operating strategy and the implementation of mitigation measures. A comprehensive monitoring strategy was employed to evaluate the strengths and limitations of these predictive tools. The paper reviews model assumptions, geotechnical data uncertainty, and operational practices to provide tangible recommendations to improve the design process.

Keywords: *block caving, reconciliation, extraction level*

1 Introduction

Block caving is a mass mining method in which an orebody is undercut to induce progressive rock mass failure and cave propagation. The caving process may be driven by gravity, stress redistribution, and/or failure along discontinuities, particularly where induced stresses exceed the strength of the rock mass or the defects within it (Duplancic & Brady 1999). Once fragmented, the ore flows by gravity and is extracted through constructed drawpoints, allowing high production tonnages to be achieved (Brannon 2011). Because of the scale of the excavations and the deformation associated with cave propagation, block caving is commonly associated with high stresses and large ground movements, particularly near the undercut and extraction levels.

A block caving mine consists of multiple levels, each playing a key role in the overall caving process (Figure 1). The extraction level serves as the primary production horizon where ore is collected through the constructed drawpoints. As the main production level, its service life must be preserved and it must remain operational through the life of the cave. The drawpoint pillars at the extraction level are particularly susceptible to elevated stress and large deformation, primarily due to cave-induced loading as the cave propagates and matures. Accordingly, the ground support system must be designed to accommodate potentially significant changes in the stress conditions over time, while providing sufficient deformation capacity and stand-up time to maintain extraction level stability and functionality.

[*] Corresponding author. Email address: john.hadjigeorgiou@utoronto.ca

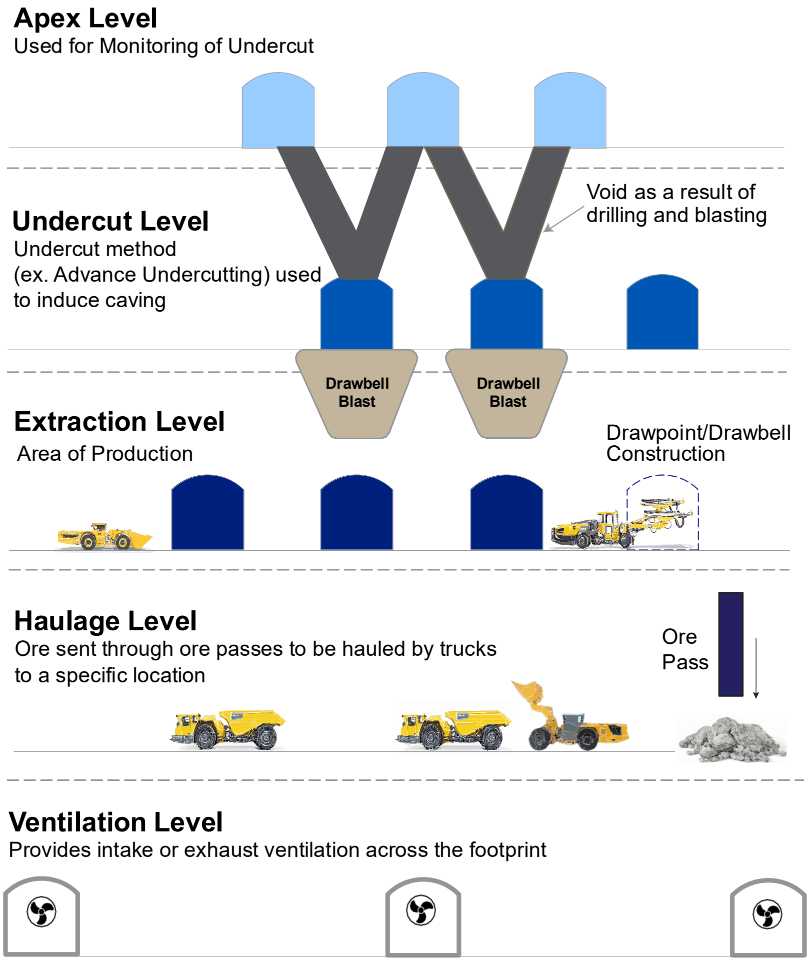

Figure 1 Block caving mine levels

A comprehensive reconciliation strategy is necessary to assess the excavation performance of an extraction level design. Reconciliation is the process of comparing planned performance to actual results using empirical monitoring data. Integrating reconciliation into the rock engineering design process can improve confidence in predictive tools by allowing models, design assumptions, and support strategies to be calibrated and refined against observed ground response. This paper presents a case study from the B3 extraction level at the New Afton Mine that links geotechnical predictions with observed performance over the life of the cave.

2 New Afton: B3 cave

The New Afton block caving mine is a copper–gold deposit located near Kamloops, British Columbia, Canada. The operation consists of 3 caves: Lift 1 (which is comprised of the east and west Panels), B3 cave, and C Zone cave (Figure 2). Lift 1 began production in 2012, with the west cave completing production in 2021 and the east cave following in 2022. TheB3 cave which began production in 2021, operated at a rate of approximately 10,500 tonnes per day and completed production in February 2026 while C Zone reached its full production rate by the fall of 2025.

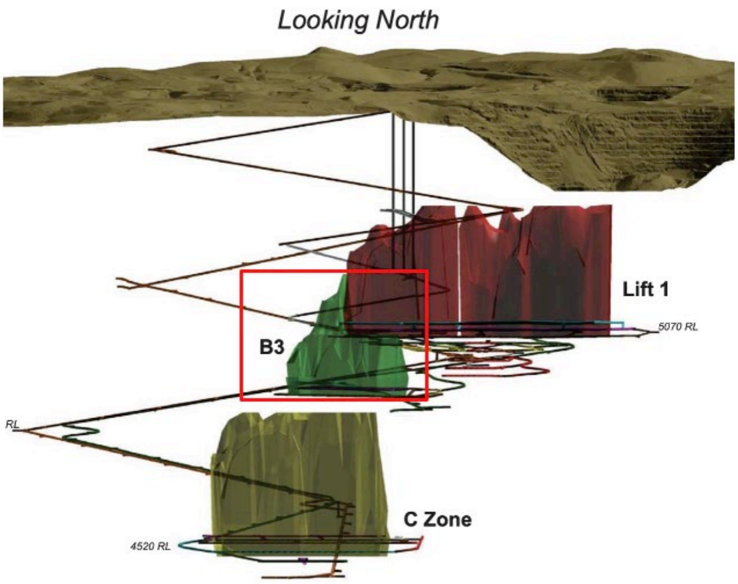

Figure 2 New Afton Mine layout

The B3 extraction footprint design employed the El Teniente layout with a total of 65 drawbells, where 24 are single-drawpoint, one-sided bells. The drawpoint spacing is 16.5 m centre-to-centre, resulting in pillars of approximately 12 m. The design was a trade-off between the successful drawpoint spacing of 15 m used in the west cave and the 18 m pillars in the east cave. The B3 extraction level is located 18 m below the undercut level. In addition, the B3 cave consists of an Apex level, located 12 m above the undercut, to assist in monitoring the undercutting performance in B3.

There are 4 lithological domains in the B3 extraction footprint: diorite, monzonite, picrite, and primary volcanic breccia (BXF) (Figure 3). BXF is predominantly seen in the footprint, with intrusions of diorite and monzonite seen towards the southeast. The extraction footprint is also intercepted by many regional faults that strike subparallel to the production drives on the outer boundaries of the extraction level (Yanagimura & Hadjigeorgiou 2022). Face mapping during the development of the extraction level identified rock mass conditions classified as a RMR89 range of 47 to 56, 'fair to poor' (Bieniawski 1988). The poorer ground was near fault structures present at the level.

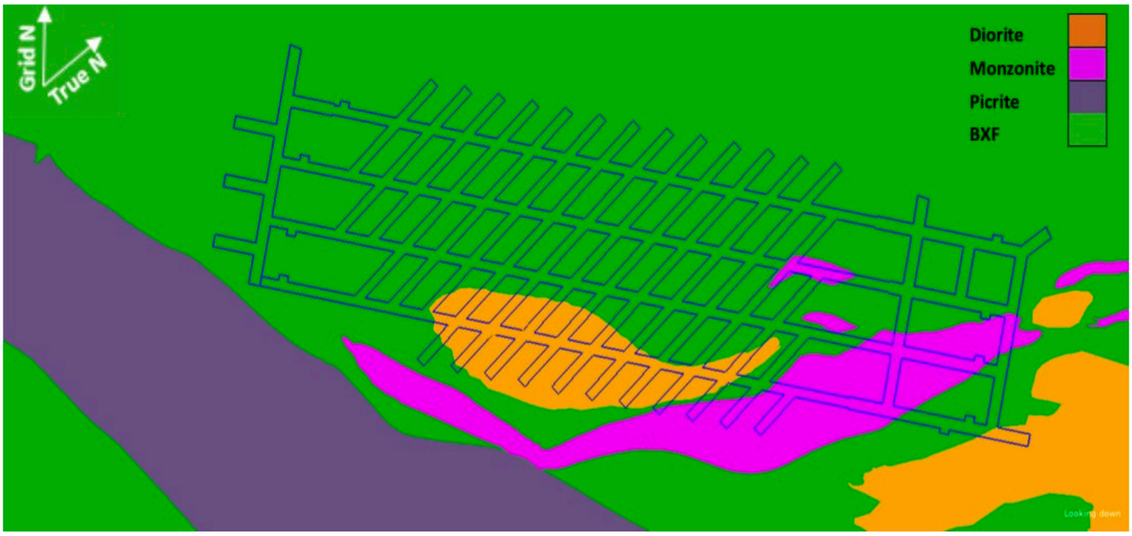

Figure 3 B3 extraction level lithological domains

3 B3 extraction level design

The design of the B3 extraction level ground support system incorporated multiple design tools, such as New Afton's pillar classification system (Yanagimura & Hadjigeorgiou 2022), empirical data from Lift 1, and numerical modelling to determine the anticipated conditions of the level over the course of the B3 cave life. The New Afton pillar classification and numerical modelling were the primary tools used to predict the anticipated conditions of the B3 extraction level.

3.1 New Afton pillar classification

A pillar classification strategy was implemented to provide further insight into the expected ground conditions and potential vulnerability that the drawpoint pillars may be exposed to. New Afton has successfully used its site-specific pillar classification system to predict the likelihood of early-onset deformation in drawpoint pillars. At B3, the initial classification of pillars was based on the regional fault model and core logging data. Ground conditions were then refined during development by collecting face mapping data. Once pillar quality was assessed based on 3 classes, ground support designs were implemented to match the anticipated ground conditions. The B3 pillar classification (Figure 4), based on ground conditions, categorised most pillars as 'very poor', indicating a high risk of early-onset deformation. The poorest conditions were observed around the perimeter of the extraction footprint, as well as in areas where major faults were near or intersected the pillars.

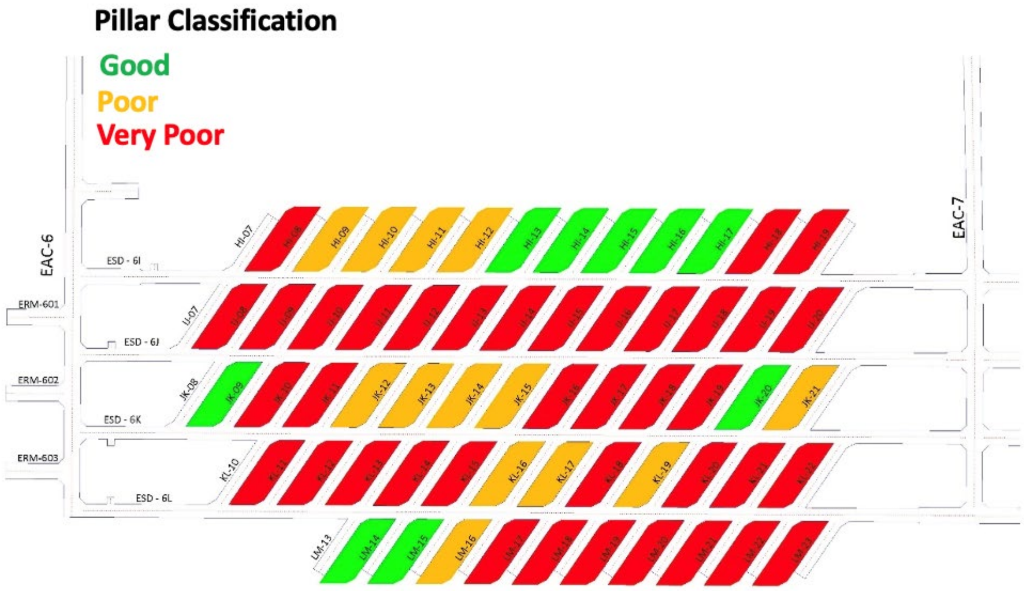

Figure 4 B3 extraction level pillar classification

3.2 Experience from Lift 1

Operational experience from Lift 1, reported by Kamp (2022), provided valuable insight into improving the design for B3's extraction level. Lift 1 began production in 2012, with mining starting from the west cave. Development moving towards the east cave was challenging due to the encountered poor ground conditions associated with major structures intersecting the east cave extraction footprint. The west cave predominantly consisted of pillars classified as 'good,' indicating a low risk of early-onset deformation. In contrast, most pillars in the east cave were classified as 'poor' to 'very poor'. As mining progressed from west to east, the deterioration in ground conditions prompted changes to the ground support design to accommodate the change in rock mass conditions (Kamp 2022). The ground support for the east cave was significantly upgraded in response to more challenging ground conditions. Short reinforcement was upgraded to higher-capacity rockbolts, replacing friction rock stabilisers (split-sets) with rebar, energy-absorbing paddle rockbolts (D-bolts), hybrid, or mechanical hybrid rockbolts. The use of higher-capacity, non-hollow rockbolts in high-stress and high-deformation areas reduced the risk of shear failure. Longer anchorage support, including 9.0 m cablebolts or self-drilling anchor rockbolts, were also installed to ensure anchorage extended beyond the depth of damage.

In addition to reinforcement support, surface support was modified through the trial of pillar wrapping using cable slings in Lift 1. This support method, commonly used at drawpoint pillars in extraction levels, provides lateral restraint and yielding capacity in high-stress environments. The Lift 1 trial demonstrated the importance of pillar confinement and led to the implementation of pillar wrapping using cable slings on the B3 extraction level for all pillars classified as 'very poor' and at high risk of deformation.

3.3 Numerical modelling

Numerical modelling is a powerful design tool and was used to predict the anticipated conditions at B3's extraction level. This aimed to evaluate the potential damage the extraction level might experience throughout the life of the B3 cave. A 3D finite difference model was used employing the ITASCA constitutive model for advanced strain softening (IMASS). Ghazvinian et al. (2020) suggest that IMASS can capture rock mass behaviour under complex stress conditions (IMASS incorporates 2 types of yielding behaviour to represent brittle rock mass response: the post-peak envelope and the ultimate strength envelope).

3.3.1 B3 extraction level stability model results

The IMASS model presents damage based on the loss of strength. The strength loss (Sloss) metric evaluates the rock mass based on the extent of softening or weakening it undergoes (Ghazvinian et al. 2020). Sloss values ranging from [-1,1] represent different stages of rock mass damage. In the model, the strength loss damage indicators were represented by 5 damage classes. The classification ranges from Class I, representing intact rock, to Class V, where the rock mass is considered caved. The remaining classes II, III and IV represent magnitudes of ground support damage. Table 1 is a reproduction of the damage classes by Cancino & Fuenzalida (2023), including Class I and Class V and the extraction level damage is referred to as 'loss defined damage classification (SDC)'.

It should be noted that the damage classes defined within the SDC framework were standard classes established through calibration at other sites and were not derived from site-specific observations collected at New Afton Mine. As these damage classes were not calibrated to the ground conditions and support practices at the B3 extraction level, their applicability was limited, although they remained useful for relating model outputs to field observations. Site-specific calibration of the damage classes is important to ensure that the framework accurately represents the observed excavation response, support performance, and progression of damage under local conditions. Without such calibration, there is a risk that the assigned damage states may either overestimate or underestimate the severity of expected ground response, reducing confidence in the framework as a tool for design, support selection, and mitigation planning. This is particularly relevant given that Ghazvinian et al. (2020) reported that underground openings with Sloss values in the range of −0.1 to −0.15 (State C) may remain stable with minimal ground support, which is inconsistent with the damage description assigned to the same Sloss range and suggests that the generic classification may not be directly applicable at New Afton.

Table 1 B3 extraction level strength loss (Sloss) damage classes (Cancino & Fuenzalida 2023)

Damage classes	Sloss values	Visible damage observations (damage mapping)	Measured deformation (LiDAR scans, borehole extensometers)	Extensometer/ observation hole survey
I	0.2 ≤ Sloss < 1.0	Less to moderate slabbing Localised bolt plates loading (up to 4) Less to moderate mesh deformation over an area >10 m^2	Less than 80 mm convergence Between 0-2 mm/day deformation rate	0.6–1.2 m depth of broken ground
II	0.0 ≤ Sloss < 0.2	High slabbing. Bolt plates loading (>4) High mesh deformation over an area >10 m^2	Between 80–12 mm convergence Between 2–4 mm/day deformation rate	1.2–1.8 m depth of broken ground
III	-0.15 ≤ Sloss < 0.0	Significant slabbing/cracking Bagging of mesh. Bolt plates yielding or cupping. One or more bolt failures. Significant mesh deformation, welds stretched or broken	>120 mm convergence >4 mm/day deformation rate	>1.8 m depth of broken ground
IV	Sloss ≤ -0.15	Drifts that have suffered larger deformations and are not serviceable anymore (without considering any rehabilitation)		
V	-1.0 ≤ Sloss < -0.15	Caved ground conditions		

The predicted Sloss damage classification at the B3 extraction level is dominated by Class III damage, characterised by significant slabbing and cracking, yielding of bolt plates, bolt failures, and extensive mesh deformation (Figure 5). The SDC model indicates that faults and cave abutment stresses are the primary controls on rock mass response, with the highest damage potential concentrated along the extraction footprint perimeter and near major faults. Class III damage is predicted adjacent to faults, including the fault along the eastern side of the footprint between production drives I and L, and around the footprint perimeter, where pillars and drives are particularly susceptible to abutment loading. The model also demonstrates the influence of the extraction layout: where half-bells are absent along the cave perimeter and production drives are exposed more directly to abutment stresses, increasing the likelihood of damage, whereas half-bells help redirect stresses away from the drives. The numerical model captures the loading cycle from extraction level development through production to end-of-life conditions. At month 51 (Figure 5), induced σ_1 stresses range from 10 to 50 MPa, with a maximum predicted value of 50 MPa.

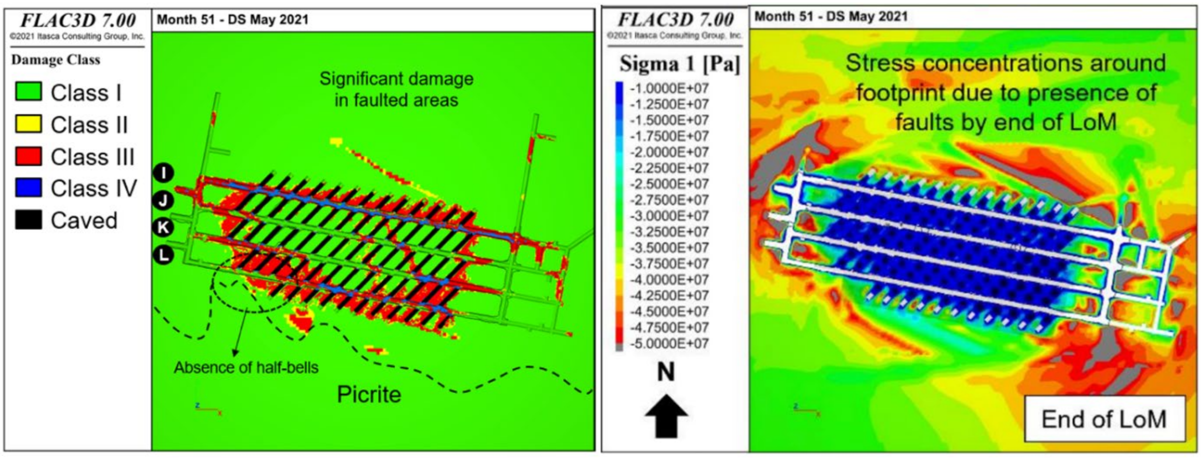

(a) (b)

Figure 5 B3 extraction level (a) strength loss defined damage classification and (b) stress model

4 Mitigation strategies

The design of the B3 extraction level incorporated findings from the New Afton pillar classification system, empirical observations from Lift 1, and predictions derived from numerical modelling. Drawing from these sources, challenging conditions were anticipated in the B3 extraction level, particularly in areas intersecting or adjacent to faults and along the perimeter of the extraction footprint. Consequently, the following mitigation strategies were implemented to address the anticipated challenges:

- Upgraded ground support system based on lessons learned from Lift 1
  - Installing higher-capacity rockbolts
  - Implementing longer anchor supports (e.g. 9.0 m cable bolts)
  - Installing pillar wrapping with cable slings in pillars classified as 'very poor'.
- Addition of half-drawbells to limit damage to the production drives as a result of the cave abutment stresses
- Compliance with a cave management plan, implementing a disciplined draw strategies
- Instrumentation program to monitor early signs of deformation (Table 2).

An extensive monitoring program was implemented in the B3 extraction level as a mitigation strategy to identify early signs of deformation. Early detection of deformation allows for minimising the need for extensive rehabilitation. At the B3 extraction level, three monitoring instruments are used: multi-point borehole extensometers (MPBX), SMART cables and LiDAR (Table 2). All instrumentation data were complemented by frequent field inspections to ensure that the data were representative of observed field conditions.

Table 2 Monitoring strategies used at the B3 extraction level (FARO Technologies Inc n.d.; MDT 2023)

Technology	Purpose	Key features	Deployment at New Afton
Convergence scans	Measure ground deformation over time	GeoSLAM scanner; practical accuracy ~10–15 mm; scan frequency depends on convergence rate	Scans are done monthly at B3 extraction level; weekly/bi-weekly in high-convergence areas; minimum 2-week interval between scans
MPBX (multi-point borehole extensometer)	Measure displacement at multiple underground points	6 anchor points per instrument; strictly a monitoring sensor (provides no ground support)	54 sensors were installed: 8 m long with 6 nodes at 1.3 m intervals along north wall, south wall, and back of production drive
SMART cables	Provide support and measure displacement	7-strand cable bolt with king wire replaced by 6-wire extensometer; strain measured via potentiometer; reduces ultimate tensile strength by ~10%	Installed as pillar wrapping at the JK-16 drawbell

5 B3 extraction level reconciliation

The availability of a comprehensive monitoring program allowed an opportunity to reconcile predictions and performance at the B3 extraction level, where production was completed in February 2026. The reconciliation of the extraction footprint is presented using the JK-16 drawbell case study. The JK-16 drawbell performance, located near the centre of the cave, was evaluated using instrumented pillar wrapping with SMART cables. This was assessed through field inspections of the individual drawpoints, J16S and K16N, and reconciled the instrumented pillar wrapping measurements.

5.1 Case study: JK-16 drawbell

The anticipated conditions for the JK-16 drawbell, as predicted by the pillar classification system and numerical model, were consistent. The pillar classification system classified the JK-16 drawbell as 'very poor' and at high risk for early-onset deformation. Similarly, the model predicted the drawbell to result in Class III damage by the end of the cave life (Figure 6). These anticipated conditions were primarily due to the presence of the B3-6 fault near the drawbell. However, the stress model did not predict high induced stresses at this location, in contrast to the other predictive approaches (Figure 6).

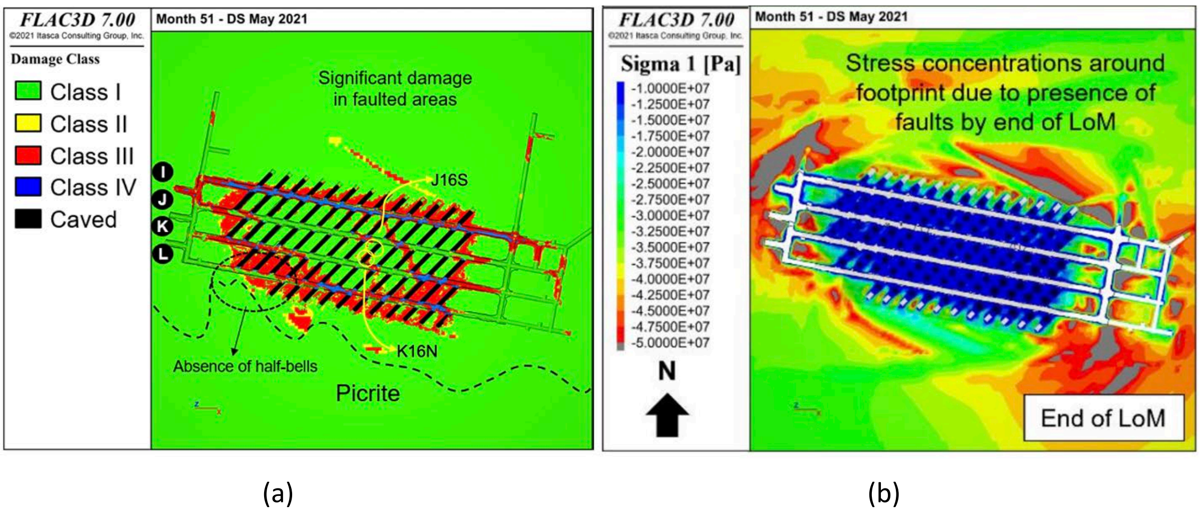

Figure 6 JK-16 drawbell anticipated conditions based on (a) strength loss defined damage classification and (b) stress model

In response to the anticipated conditions, the mine implemented a series of mitigation strategies. The ground support design for the drawbell followed the protocol for pillars classified as 'very poor'. Primary support system included fibre-reinforced shotcrete, reinforcement elements such as MD rockbolts or D-bolts, and welded wire mesh. Secondary support consisted of 3 rows of pillar wrapping using cable slings, a row of hollow bar rockbolts, OSRO straps, and a second application of fibre-reinforced shotcrete. For monitoring, the pillar wrapping was instrumented with SMART cables to monitor pillar deformation over time and evaluate the effectiveness of the support strategy as the cave matures.

Throughout the duration of the cave life, the field inspections identified minimal signs of damage on the drawpoint pillars. Figure 7 presents the ground conditions at the J16S and K16N drawpoints as of October 2025. The J16S drawpoint minor damage was observed on the pillars, which did not indicate signs of deformation and was likely due to equipment contact. However, the fibre-reinforced shotcrete layer may hide visible signs of pillar deformation.

Figure 7 J16S drawpoint conditions at the end of B3 cave life

Each drawpoint bullnose and camelback pillar was installed with 3 rows of instrumented cable sling pillar wrapping. A total of 12 SMART cables were installed at the drawpoint, of which 5 remained active as of October 2025. The loss of instruments is attributed to equipment contact, cable failure, or installation issues. Routine J16S field inspections identified minimal pillar damage, with no observable deformation and minor damage likely caused by equipment contact (Figure 7), contrary to predictions from the numerical model and pillar classification system. Displacement data for the J16S bullnose and camelback pillars over approximately 3.5 years (Figures 8 and 9) show minimal movement following the initial drawbell blasts at JK-16 and JK-17 in May and June 2022. Overall pillar displacement did not exceed 2 mm.

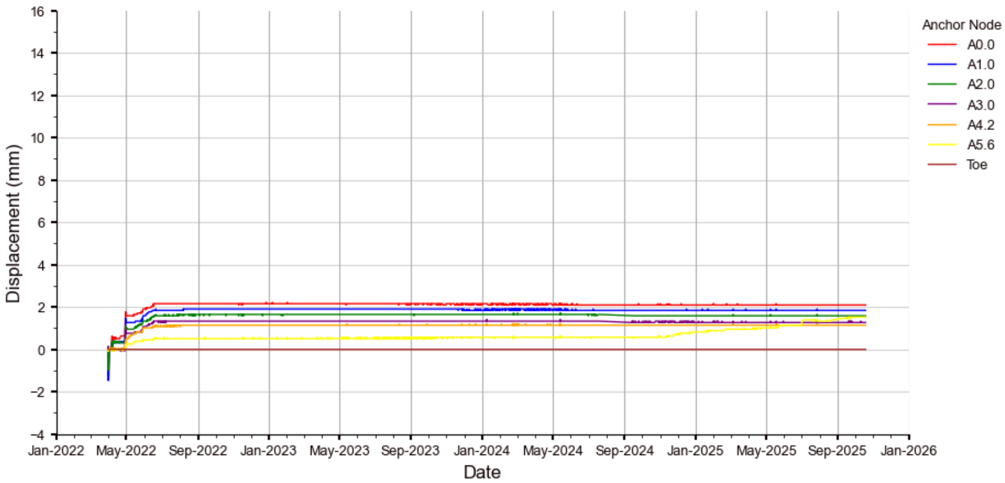

Figure 8 J16S bullnose, production drive side, top row instrumented cable sling

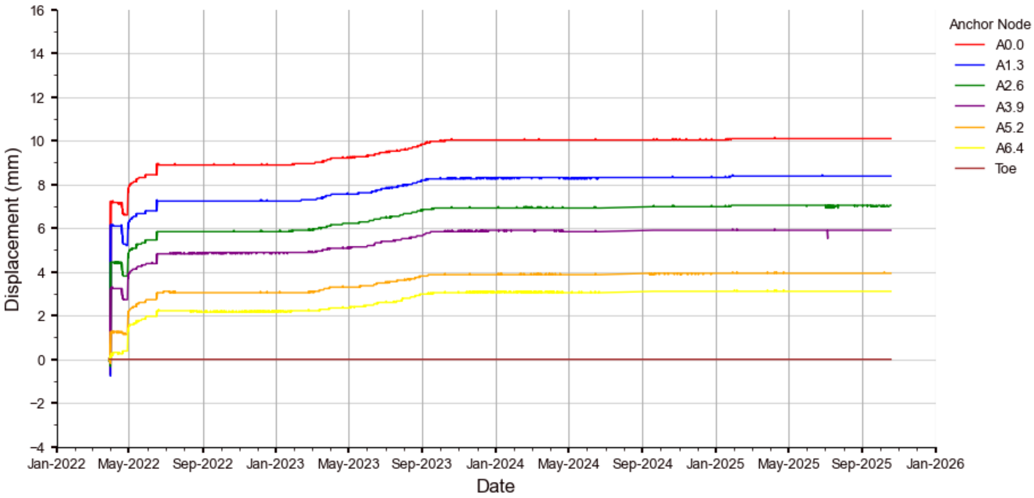

Figure 9 J16S camelback, drawpoint side, top row instrumented cable sling

The K16N bullnose and camelback pillar wrapping, similar to J16S, did not exhibit an increase in displacement until January 2025. Field inspections conducted in February 2025 revealed no significant signs of damage at K16N (Figure 10). Overall, the ground conditions at the drawpoint were good. The fibre-reinforced shotcrete layer showed minimal or no fracturing, and the drawpoint brow remained intact with no visible damage to the steel sets. No ground support damage was observed. The back of the drawpoint appeared relatively flat, with no visible 'hummocks' or other indicators of stress-related deformation. However, between February and October 2025, ground conditions at the K16N drawpoint deteriorated, with the first signs of damage observed in June 2025, indicating elevated stress conditions. The drawpoint transitioned from no visible damage to widespread shotcrete cracking, with slabs peeling from the brow and exposing the steel set.

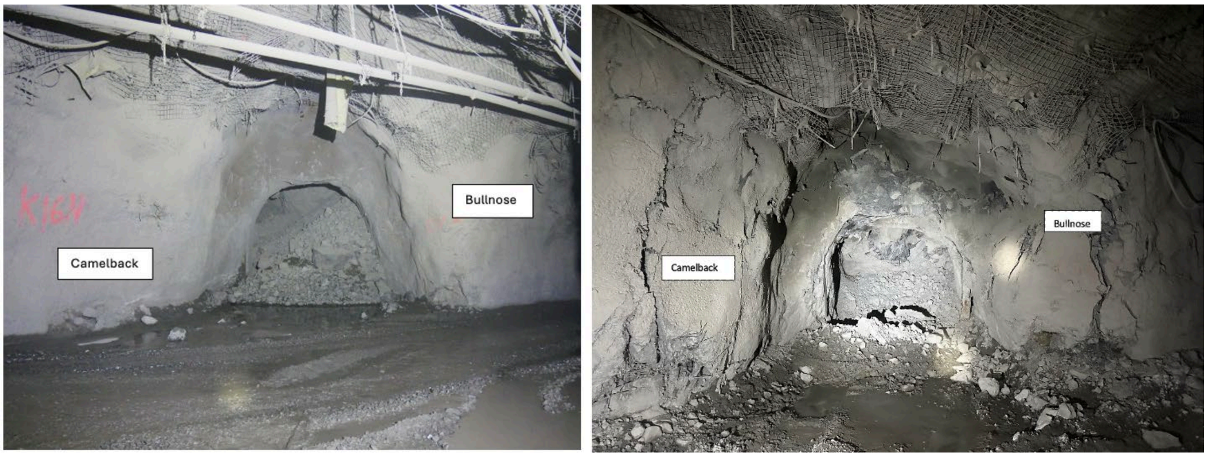

(a) (b)

Figure 10 K16N drawpoint conditions in (a) January 2025 to (b) October 2025

Beginning January 2025, a gradual increase in displacement was detected by the instrumented cable slings on the bullnose and camelback pillar (Figures 11 and 12). The bullnose pillar production side monitoring data displayed an increase in displacement of 35 mm. The camelback pillar displayed an increase in displacement of 5 mm from March 2025.

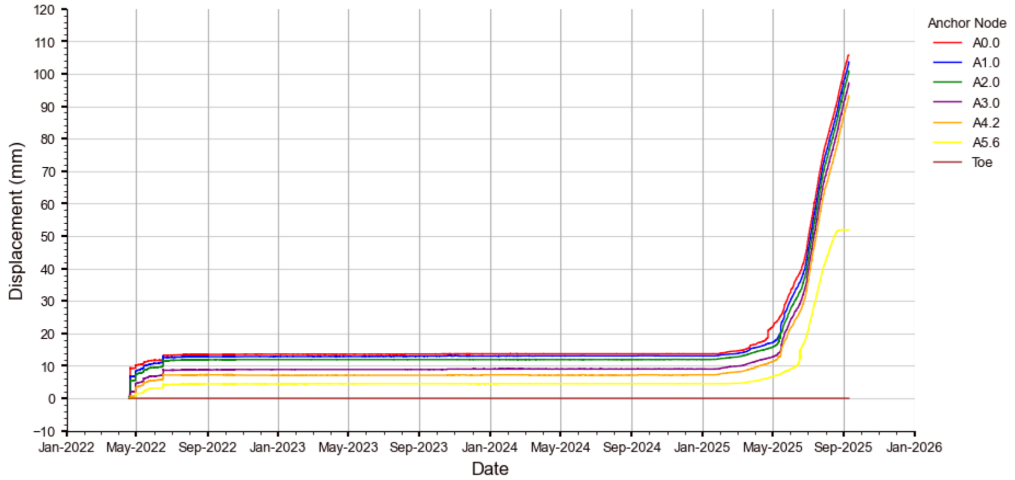

Figure 11 K16N bullnose, production drive side, bottom row instrumented cable sling

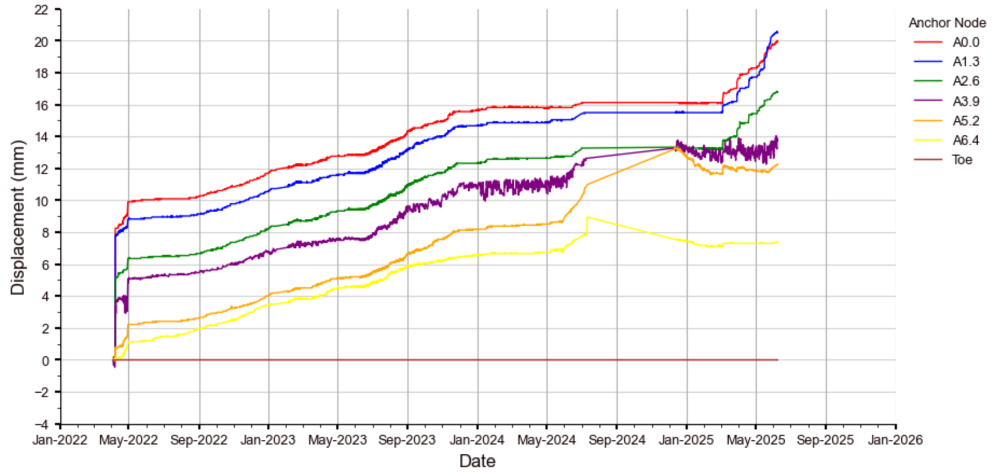

Figure 12 K16N camelback, drawpoint side, middle row instrumented cable sling

The increase in displacement recorded by the instrumented cable slings was consistent with underground observations. Pillar conditions were characterised by extensive fracturing of the fibre-reinforced shotcrete, including fractures up to 2 m long where reinforcing fibres were no longer engaged. The bullnose pillar exhibited exposed rock surfaces due to shotcrete delamination (Figure 10). Delamination at the back of the drawpoint and along the production drive side of the bullnose pillar created an uneven profile and caused shotcrete to fall onto the screen, straining the mesh. This deformation-related damage is believed to have led to the loss of the bullnose and camelback pillar monitoring instruments in June and September 2025, respectively, as no data were recorded beyond those dates (Figures 11 and 12).

6 Reconciliation

The New Afton pillar classification system identified the JK-16 drawbell as a 'very poor' pillar, prompting additional long support at tighter spacing and deformation-tolerant surface support, including cable sling pillar wrapping and OSRO straps. All 'very poor' pillars at B3 received cable sling wrapping, while both drawpoints were supported with higher-capacity rockbolts, longer secondary support, and pillar wrapping based on Lift 1's East Cave experience.

The Sloss Damage Classification predicted Class III damage for JK-16, particularly at K16N. At J16S, minimal pillar deformation was recorded by SMART cable from 2021 to 2025, requiring no rehabilitation. K16N, however, required early rehabilitation due to overbreak near intersecting faults. Later stages showed shotcrete delamination and bagging at the back near the bullnose pillar; rehabilitation was deprioritised as production declined. Overall, JK-16 monitoring data indicated that installed support was effective.

In terms of the influence of mining activity, draw control is critical in block caving, influencing fragmentation, stress distribution, and cave loading. Variations in draw rate can alter cave loading and contribute to deformation at the extraction level. The relationship between draw rate and convergence has been well documented at block caving operations such as PT Freeport and Northparkes (Rubio et al. 2011; Febrian et al. 2004; Snyman & Webster 2022). At Northparkes, both excessive and insufficient ore extraction were observed to initiate convergence (Snyman & Webster 2022). At PT Freeport, an inverse relationship between convergence and draw rate was reported, with consistent draw corresponding to a steady convergence rate (Febrian et al. 2004). Consequently, maintaining a uniform and consistent extraction rate, rather than prioritising ore grade, can assist in controlling convergence within an area. Deformation at K16N increased in January 2025, coinciding with a decline in draw compliance from April 2025 due to hangups, oversize material, and reduced draw rates due to decreasing ore grade (Figure 13).

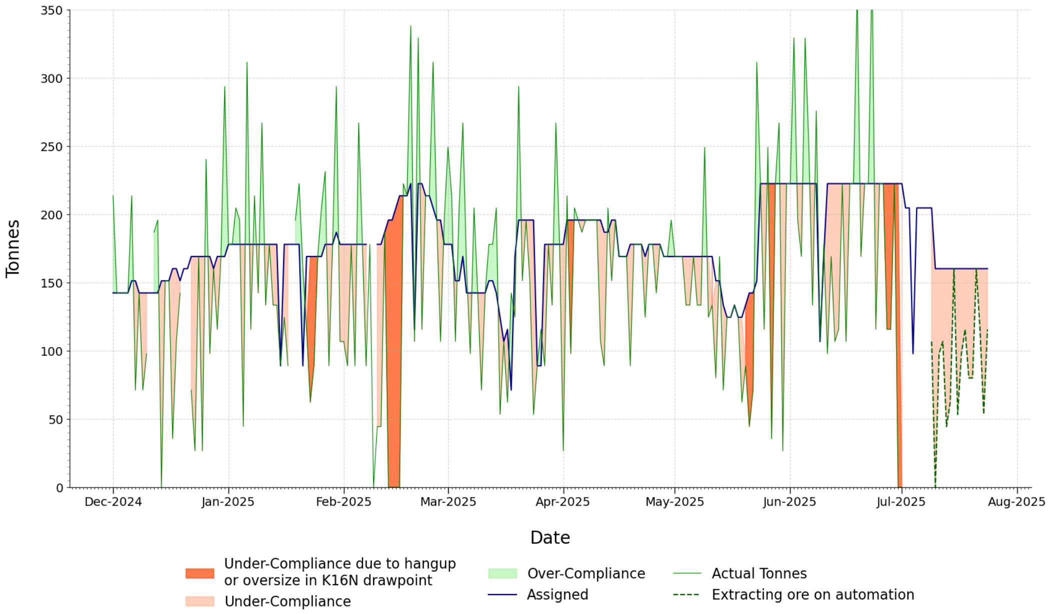

Figure 13 K16N draw compliance January to August 2025

Ore grade fluctuations commenced in early January 2025. Gold grades began to decline in early May 2025, with both gold and copper grades decreasing markedly by August 2025. This trend is consistent with the mature stages of a cave, where grade dilution commonly occurs later in cave life as a result of sustained, uniform draw and the progressive smoothing of the ore–waste interface (Laubscher et al. 2016).

An additional contributor to the reduced draw rate was poor ground conditions at the K16N drawpoint, where loose material accumulated at the back, placing strain on the mesh. To reduce personnel exposure, ore extraction at K16N was transitioned to automated mucking on 3 July 2025. At the B3 extraction level, automated mucking is restricted to shift changes, resulting in approximately 2–3 hours of mucking per day (Figure 13). The reduction in draw beginning in January 2025 likely contributed to the increased deformation observed at K16N. Low draw rates are recognised as promoting time-dependent failure, as drawpoints remain subject to sustained muck pile loading and arching stresses (Laubscher et al. 2016). Overall, excavation performance indicates that the mitigation strategies were more effective than predicted by the numerical model and the New Afton pillar classification system.

7 B3 extraction level lessons learned

Reconciliation between predictive tools and observed conditions at the B3 extraction level highlighted differences between predicted and observed performance. The numerical model predicted high induced stresses of 40–50 MPa around the extraction level perimeter and comparatively low stresses of approximately 10 MPa within the footprint, with the elevated perimeter stresses attributed to abutment loading around the cave margin. The damage model predicted significant ground support damage along the perimeter and within the footprint, where pillars were affected by fault material. Similarly, the New Afton pillar classification system indicated a high risk of deformation, with most pillars classified as 'very poor' or 'poor' due to the presence of east–west striking regional fault structures.

Underground observations supported by SMART cable instrumentation at the JK-16 drawbell revealed that actual performance differed from these predictions. Low stress conditions within the extraction level were consistent with the observed behaviour at the J16S drawpoint, where minimal deformation and no stress-induced damage were recorded throughout the majority of the cave life. The K16N drawpoint also remained stable for most of the production period, with notable deformation occurring only near the end of cave life when draw rates began to fluctuate.

The difference between predicted and observed performance suggests that the treatment of faulted ground within the predictive frameworks was overly conservative for the B3 extraction level. In both the numerical modelling and empirical classification approaches, fault-affected areas were generally interpreted as being at elevated risk of damage and deformation. However, field observations indicate that not all drawpoints associated with major fault structures performed poorly. This suggests that simplifying fault behaviour across the extraction level, including the assumption that major faults represent uniformly weak or highly adverse ground conditions, may have contributed to the overclassification of drawpoints as being at high risk of deformation.

This interpretation is particularly relevant to the SDC results which predicted a broader extent of damage than was observed in the field. Additional uncertainty may also have arisen from the simplified representation of structural geology in the numerical model, in which all major faults were assigned a uniform uniaxial compressive strength of 24 MPa despite likely variability in fault composition, architecture, and mechanical behaviour. Similarly, the effectiveness of the New Afton pillar classification system depends strongly on the quality of the lithological and structural inputs used. In hindsight, it would have been beneficial to update the B3-specific geotechnical input data, rather than relying on parameters carried forward from Lift 1, particularly within the fault domain.

A key finding from this case study is that deformation was not controlled by the presence of faulting alone. Rather, drawpoints that experienced poorer performance were generally those located near or intersected by fault structures and subjected to adverse operational conditions, including inconsistent draw. Faulting contributed to challenging development conditions, overbreak, and difficulty installing ground support, which likely reduced the robustness of the excavations from the outset. However, significant deformation was not observed until later in cave life, when draw rates became irregular. This indicates that structural complexity increased vulnerability, but that deformation expression was strongly influenced by operational factors, particularly draw control. These findings highlight the importance of maintaining uniform draw rates, especially where excavation performance may already be sensitive to local ground conditions.

With respect to ground support, pillar wrapping using cable slings was installed on all pillars classified as 'very poor' at the B3 extraction level based on the anticipated ground conditions. The performance of this support system was evaluated using SMART cable instrumentation installed within the pillar wrapping at the JK-16 drawbell to assess long-term behaviour. The pillar wrapping exhibited minimal displacement throughout most of the cave life, with increased movement observed only during periods of fluctuating production rates near the end of cave life. Although several SMART cable instruments were lost due to equipment interaction and deformation, the available quantitative data, supported by field observations, indicate that the pillar wrapping strategy performed effectively. Notably, the majority of pillars classified as 'very poor' across the B3 extraction level did not exhibit significant deformation, supporting the conclusion that the adopted support approach met the design intent under the conditions encountered.

Future instrumentation programs should incorporate greater redundancy, as the loss of multiple SMART cable instruments at JK-16 highlighted the vulnerability of individual sensors to operational damage and deformation. More broadly, this case study demonstrates the importance of site-specific reconciliation to refine predictive tools, improve representation of fault behaviour, and distinguish between areas of genuinely elevated deformation risk and areas that may be conservatively classified due to simplified geological assumptions.

8 Conclusion

The completion of the B3 cave provided an opportunity to reconcile anticipated ground conditions with observed excavation performance, evaluate the effectiveness of the predictive tools applied at the B3 extraction level, and assess the performance of the mitigation strategies implemented. Overall, the B3 extraction level performed better than initially anticipated, as demonstrated by the JK-16 drawbell case study, which confirmed the effectiveness of the mitigation measures and indicated that deformation was less severe and less widespread than predicted. Instrumented pillar wrapping data, supported by underground observations, validated the general stability of the excavation through most of the cave life and provided valuable insight into the conditions under which deformation developed.

The key outcome of the reconciliation was not simply the identification of differences between predicted and observed performance, but a better understanding of the factors contributing to those differences and how they can be incorporated into future designs. In particular, the results suggest that the treatment of faulted ground within the predictive frameworks was likely overly conservative for B3. Simplified representation of the fault domain, including the use of parameters carried forward from previous lifts and the assumption of consistently poor fault-related ground conditions, may have contributed to overclassification of deformation risk in both the empirical and numerical assessments. While faulting clearly influenced excavation performance and ground support installation conditions, field observations showed that not all drawpoints associated with major fault structures experienced poor performance. Accordingly, a key recommendation for future work at New Afton is to improve site characterisation of the fault domain, while also refreshing the broader geotechnical domain inputs rather than carrying forward parameters from other lifts without reassessment. More detailed characterisation of lithology, fault architecture, and associated rock mass conditions would support better-calibrated empirical classifications and more representative numerical modelling inputs. This would improve confidence that future design assessments reflect the actual variability of ground conditions present at the extraction level.

The reconciliation also highlighted the need to improve how model outputs are translated into information that is meaningful and usable at site. The use of SDC damage classes to relate model results to expected field performance is only effective if those damage classes are calibrated to site-specific excavation response, ground support performance, and observed damage progression. At B3, the direct linkage of Sloss values to damage classes did not capture the extent of rock mass and ground support damage under New Afton conditions. In addition, where ground support response is not explicitly modelled, the relationship between Sloss and observed support damage is necessarily simplified and subject to inherent limitations. These limitations should be clearly acknowledged when applying the approach.

Overall, the B3 case study demonstrated the value of reconciliation as a tool for improving future design practice. The lessons learned from B3 indicate that better local characterisation, particularly of the fault domain, together with improved site-specific calibration of model output to observed excavation behaviour, would strengthen the reliability and practical usefulness of predictive tools for future extraction level design at New Afton.

Acknowledgement

The authors acknowledge the collaboration and support of New Afton management and the technical and operating team. The views and opinions presented in the article are the authors’ own and do not reflect any position or outlook of Coeur New Afton.

References

Bieniawski, ZT 1988, 'The rock mass rating (RMR) system (geomechanics classification) in engineering practice', in L Kirkaldie (ed.), *Rock Classification Systems for Engineering Purposes*, ASTM STP 984, American Society for Testing and Materials, Philadelphia, pp. 17–34.

Brannon, CA, Carlson, GK & Casten, TP 2011, 'Block caving', in P Darling (ed.), *SME Mining Engineering Handbook*, 3rd edn, Society for Mining, Metallurgy, and Exploration, Littleton, pp. 1437–1451.

Cancino, C & Fuenzalida, M 2023, *Caving Analysis of B3 Cave at New Afton Mine*, Report no. 2-5706-07:23R53, ITASCA, Minneapolis.

Duplancic, P & Brady, BH 1999, 'Characterisation of caving mechanisms by analysis of seismicity and rock stress', in G Vouille & P Berest (eds), *Proceedings of the 9th International Congress on Rock Mechanics*, A.A. Balkema, Rotterdam, pp. 1049–1053.

FARO Technologies Inc n.d., *GeoSLAM ZEB Horizon RT Mobile Scanner*, https://www.faro.com/en/Products/Hardware/GeoSLAM-ZEB-Horizon-RT

Febrian, I, Yudanto, W & Rubio, E 2004, 'Application of convergence monitoring to manage induced stress by mining activities at PT Freeport Indonesia Deep Ore Zone Mine', in *Proceedings of MassMin 2004*, Instituto de Ingenieros of Chile, Santiago, pp. 269–272.

Ghazvinian, E, Garza-Cruz, T, Bouzeran, L, Fuenzalida, M, Cheng, Z, Cancino, C & Pierce, M 2020, 'Theory and implementation of the Itasca constitutive model for advanced strain softening (IMASS)', in *MassMin 2020: Proceedings of the Eighth International Conference & Exhibition on Mass Mining*, University of Chile, Santiago, pp. 451–461.

Kamp, C 2022, 'Management of production drift convergence and redevelopment', in Y Potvin (ed.), *Caving 2022: Proceedings of the Fifth International Conference on Block and Sublevel Caving*, Australian Centre for Geomechanics, Perth, pp. 831–848, https://doi.org/10.36487/ACG_repo/2205_57

Laubscher, DH, Guest, A & Jakubec, J 2016, *Guidelines on Caving Mining Methods: The Underlying Concepts*, University of Queensland, Brisbane.

MDT 2023, *SMART MPBX Installation Instructions*, manual, https://mdt.ca/wp-content/uploads/2023/02/smart_cable_installation_instructions1.pdf

Rubio, E, Widijanto, E & Bayuargo, M 2011, 'Damage prediction in the extraction level of block caving mine – Case study in Deep Ore Zone Mine, PT Freeport Indonesia', in *Proceedings of the 45th U.S. Rock Mechanics/Geomechanics Symposium*, American Rock Mechanics Association, Alexandria.

Snyman, L & Webster, S 2022, 'Northparkes E48 block cave: the mining history of a successful block cave', in Y Potvin (ed.), *Caving 2022: Proceedings of the Fifth International Conference on Block and Sublevel Caving*, Australian Centre for Geomechanics, Perth, pp. 95–108, https://doi.org/10.36487/ACG_repo/2205_04

Yanagimura, Y & Hadjigeorgiou, J 2022, 'A monitoring strategy to assess the effectiveness of pillar wrapping', in Y Potvin (ed.), *Caving 2022: Proceedings of the Fifth International Conference on Block and Sublevel Caving*, Australian Centre for Geomechanics, Perth, pp. 501–516, https://doi.org/10.36487/ACG_repo/2205_34